Rottlerin-Liposome Inhibits Endocytosis of Feline Infectious Peritonitis Virus Infection Through PKCδ Dependent Manner

Jong-Chul Choi , Sung-Won Jung , In-Yeong Choi , Yeong-Lim Kang , Dong-Hun Lee , Sang-Won Lee , Seung-Yong Park , Chang-Seon Song , In-Soo Choi , Joong-Bok Lee , Changin Oh *

Posted Date: 7 April 2023

doi: 10.20944/preprints202304.0106.v1

Keywords: Feline Infectious Peritonitis; Rottlerin; Drug Delivery System; Liposome; Antivirals

Article

Rottlerin-Liposome Inhibits Endocytosis of Feline Infectious Peritonitis Virus Infection through PKCδ Dependent Manner

Jong-Chul Choi [1,2], Sung-Won Jung [2], In-Yeong Choi [2], Yeong-Lim Kang [2], Dong-Hun Lee [2,3], Sang-Won Lee [2,3], Seung-Yong Park [2,3], Chang-Seon Song [2,3], In-Soo Choi [2,3], Joong-Bok Lee [2,3] and Changin Oh [4,*]

[1] Qvet Co. Ltd., 606, Alumini Association Building of Konkuk University, 5, Achasan-ro 36-gil, Gwangjin-gu, Seoul 05066, Republic of Korea; mfilia@konkuk.ac.kr (J.-C.C.)
[2] Laboratory of Infectious Diseases, College of Veterinary Medicine, Konkuk University, 120 Neungdong-ro, Gwangjin-gu, Seoul 05029, Korea; tjddnjs0204@naver.com (S.-W.J.); joealpha@naver.com (I.-Y.C.); vinlovehole@naver.com (Y.-L.K.)
[3] KU Research Center for Zoonosis, 120 Neungdong-ro, Gwangjin-gu, Seoul 05029, Republic of Korea
[4] Department of Genetics, Yale School of Medicine, PO Box 208005, New Haven, CT 06520-8005, USA; changin.oh@yale.edu (O.C.)
* Correspondence: changin.oh@yale.edu

Simple Summary: Rottlerin, a type of natural extract, can inhibit the activity of various viruses. Feline infectious peritonitis virus (FIPV) causes a devastating disease in cats, but no prevention or treatment methods have been established. We investigated whether Rottlerin has inhibitory effects on FIPV. In this study, we demonstrated that Rottlerin inhibits FIPV replication and exerts PKCδ-related action. We showed that Rottlerin affects the early (endocytosis) and late (syncytium formation) stages of FIPV replication. We also observed that the liposome encapsulation technique overcomes the drawbacks of Rottlerin and enhances its efficacy. Therefore, we suggest that Rottlerin-Liposome has worth to be developed as a potential therapeutic agent for FIPV.

Abstract: Rottlerin(R) is a natural extract from *Mallotus philippensis* with antiviral properties. Feline Infectious Peritonitis (FIP) is a fatal disease characterized by systemic granulomatous inflammation and high mortality, with no established prevention or cure. We investigated antiviral effect of liposome loaded R, Rottlerin-liposome(RL) against Feline infectious peritonitis virus (FIPV), the causative agent of FIP. We demonstrated that RL inhibited FIPV replication in dose dependently with a PKCδ related manner, not only in the early endocytosis step but also in the late step of replication. RL resolved the low solubility issue of rottlerin and improved its inhibition efficacy at the cellular level. Based on these findings, we suggest that RL has a value for further research as a potential antiviral agent against FIPV.

Keywords: Feline Infectious Peritonitis; Rottlerin; Drug Delivery System; Liposome; Antivirals

1. Introduction

Rottlerin(R) is a natural polyphenol ketone compound derived from the powder of *Mallotus philippensis*, commonly known as Kamala tree, which has been traditionally used as a food additive and a folk remedy to treat mild enteric diseases [1–3]. R has been widely used as a protein kinase C δ(PKCδ) specific phosphorylation inhibitor [4–6]. R is also known to possess several medicinal properties such as anticancer, anti-inflammatory, antioxidant, and hepatoprotective effects [7,8]. Intriguingly, several studies demonstrated that R has inhibitory activity against various pathogens, including parasite, bacteria, and viruses [4,5,8–13].

A drug delivery system (DDS) has been widely used in various field to increase the efficacy of pharmaceutical substances [14–16]. Among them, a liposome have advantages in improving the solubility, delivery efficiency, and storage stability of substances [17–19]. Liposome technology has

 doi:10.20944/preprints202304.0106.v1

been applied to natural extracts to solve their original problems including high hygroscopic structure, low solubility, poor bioavailability, instability, and high-dose-induced toxicity [19,20]. Good examples of liposome applied natural extracts to pharmaceutical substances are curcumin, fat-soluble vitamins, and polyphenols from tea [21–23].

Feline infectious peritonitis virus (FIPV) is a known causative agent of a devastating disease, Feline Infectious Peritonitis (FIP), characterized by systemic granulomatous inflammation [24,25]. FIPV developed from the major biotype of feline coronavirus, Feline enteric coronavirus (FeCoV) (Order: *Nidovirales*, Subfamily: *Coronavirinae*, Family: *Coronaviridae*), which gains tropism for macrophages by mutations occurred in the Spike protein [25,26]. Clinically, FIP comes in two forms: wet and dry [27]. [27]Both forms cause granulomatous lesions consisting of macrophages and other inflammatory cells in multiple organs such as the omentum, mesenteric lymph nodes, spleen, and liver [28]. Clinical symptoms include fever, jaundice, abdominal effusions, weight loss, and may also affect the eyes and central nervous system [27,29]. Once clinical symptoms occur, the mortality rate is almost 100%, and expected survival timer after diagnosis is reported to be 8-9 days [27,30,31]. Even in cases where apparent recovery has occurred, symptoms may recur several months to several years later [32].

Controlling and treating infections with FIPV is almost impossible due to its epidemiological characteristics. FeCoV primarily infects kittens during the nursery period and causes mild enteric disease [24,33]. Therefore, early management, such as separating young cats from their queen, is necessary to prevent the infection and development to FIP[33,34]. The lack of effective prevention measures and the absence of any cure other than supportive therapy makes the situation even more challenging [27,33]. There are several antiviral candidates for FIPV, including Chloroquine, GS-441524, Ribavirin, GC376, U18666A, Itraconazole, which have undergone animal or clinical trials [29,35–39]. However, a drug that is suitable for use as a therapeutic agent in clinic has not yet been developed [40].

Previously, our group demonstrated that Rottlerin-liposome (RL), liposome encapsulated rottlerin, successfully inhibited porcine reproductive and respiratory syndrome virus (PRRSV) infection in piglet [4]. Thus, we hypothesized that FIPV, which is in same order of PRRSV, is also able to be inhibited by RL. In this study, we revealed that RL inhibited the replication of FIPV. The early anti-FIPV effect of RL is related to PKCδ phosphorylation. RL affects at least two steps of FIPV replication, one at an early endocytosis of FIPV and other at the late step, which possibly related to syncytia formation step. Our study provides preliminary evidence the inhibitory effect of RL on FIPV and its possible mechanism, and highlights the potential advantages of applying liposomes to antiviral drugs.

2. Materials and Methods

2.1. Cell, Virus, and Antibodies

In this study, we used WSU 79-1146 (VR-990) virus as a model for FIPV [41]. Crandell feline kidney (CRFK) cells were grown according to ATCC handling guidelines for the virus. The cells were maintained using Eagle's Minimum Essential Medium (EMEM) with 10% fetal bovine serum (FBS) and 1% Antibiotic-Antimycotic solution, and the concentration of FBS was changed to 2% for the virus propagation. For immunofluorescence assay and Western blot, mouse anti-FIPV nucleocapsid (N) IgG, clone FIPV3-70 (BioRad, Hercules, CA, USA), PKCδ (D10E2) Rabbit mAb (Cell Signaling Technology, Danvers, MA, USA), Anti-PKC delta (phospho S645) antibody (Abcam, Cambridge, MA, USA), and Goat anti-Rabbit IgG (H+L), HRP (Thermo Fisher Scientific, Cleveland, OH, USA), Goat anti-Mouse IgG (H+L), Alexa Fluor 488 (Thermo Fisher Scientific, Cleveland, OH, USA) or Goat anti-Mouse IgG, HRP (Abcam, Cambridge, MA, USA) were used [4,42,43]. Anti β-actin antibody, HRP (Abcam, Cambridge, MA, USA) was used for β-actin staining in Western blot.

Preprints (www.preprints.org) | NOT PEER-REVIEWED | Posted: 7 April 2023 doi:10.20944/preprints202304.0106.v1

2.2. Preparation of the R and the RL

R was dissolved in dimethyl sulfoxide (DMSO) at a concentration of 10 mg/ml. RL was prepared by thin-film hydration method with reference to the previous study [4,18]. Hydrogenated soy phosphatidylcholine (HSPC) and Cholesterol in a ratio of 55: 45 (mol/mol) were added to a flask containing an ethyl acetate (1:2 v/v). Then, R was added in 1/20 of the weight of the mixture. The mixture was dissolved by stirring at room temperature for 1 hour, the flask was mounted on a rotary evaporator (WIGGENS, Straubenhardt, Germany), and the device was operated under conditions of 54 °C, 50 rpm, and 300 mbar to form a thin layer of film on the surface of the flask. DW was added to hydrate the layer at 65 °C and 60 rpm. After the film was fully hydrated, the recovered product was dialyzed against DW overnight at room temperature.

2.3. Characterization of the RL

To verify the quality of the RL, we measured the shape, size, and concentration of RL. The shape of the particles was evaluated by utilizing a transmission electron microscope (TEM), while the size distribution was determined using a dynamic light scattering (DLS) system (Wyatt Technology, Santa Barbara, CA, USA). To determine the amount of R encapsulated in liposome, triton-x100 was mixed with the prepared RL in a ratio of 19:1 to dissolve the lipid (v/v), and the absorbance was measured at a wavelength of 405 nm using a spectrophotometer (TECAN, Männedorf, Switzerland) [44]. The absorbance values obtained were converted to concentration using a standard curve.

2.4. Cell Viability Assay

Twenty-four hours prior to the test, CRFK cells were seeded at a concentration of $2x10^5$ cells/mL in 96-well plates. Various concentrations of R and RL (Fig. 1A) were prepared by diluting them with a cell culture medium, and 100 μL of each concentration was added to the wells. DMSO was added as a control. The plates were then incubated at 37 °C in 5% CO_2 for 48 hours. Following this, 10 μL of EZ-Cytox (Water Soluble Tetrazolium Salts) solution (Daeil Lab Service, Seoul, Korea) was added to each well and further incubated for 4 hours [4]. At the end of the incubation period, the optical density of the wells was measured at a wavelength of 450 nm using a spectrophotometer (TECAN, Männedorf, Switzerland). The optical density value of the control group was considered as 100%, and each value was normalized accordingly.

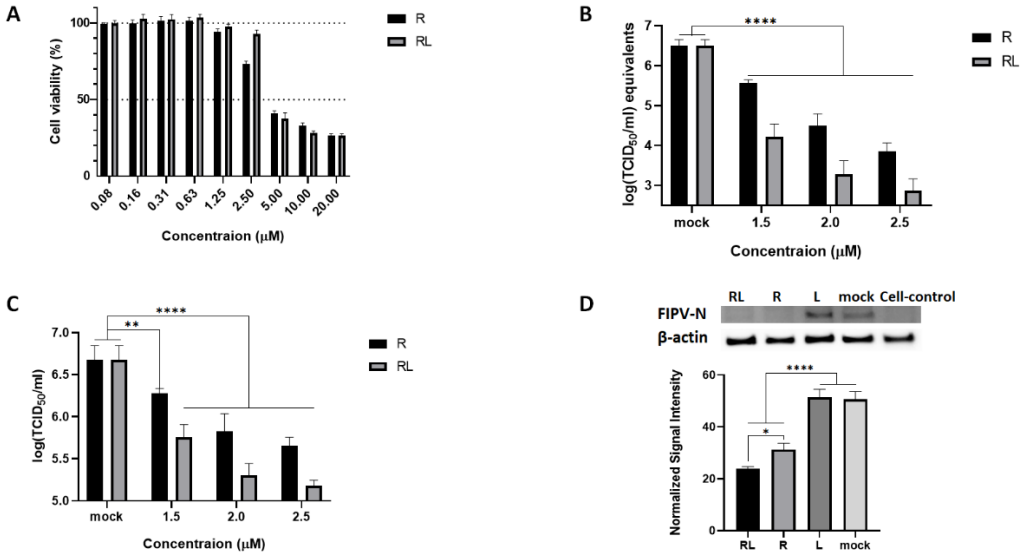

Figure 1. The RL inhibited FIPV replication in a dose-dependent manner. (A) Confluent CRFK cells were treated with R and RL at indicated concentrations and incubated for 48 hours. After that, cell viability was measured by MTT assay. **(B and C)** Pre-treated (Indicated concentration of R or RL) CRFK cells were infected with FIPV(MOI = 0.008) with R or RL for 1 hours, followed by same R or

Preprints (www.preprints.org) | NOT PEER-REVIEWED | Posted: 7 April 2023 doi:10.20944/preprints202304.0106.v1

RL treatment up to 72hpi. Amount of virus was measured by RT-qPCR (B) and titration (C). **(D)** Confluent CRFK cells were infected with FIPV (MOI = 0.008) with R(2.5μM) or RL(2.5μM), or liposome. At 24 hour post infection, cell lysates were examined by Western Blot and the intensity of the bands was quantified by Image J and normalized to the value of β-actin. The statistical differences were analyzed by one-way ANOVA and Dunnett's multiple comparison. The symbols (****), (**) and (*) indicate $p<0.0001$, $p<0.005$ and $p<0.05$, respectively.

2.5. Dose-Dependent Inhibition Assay

The CRFK cells were seeded at a concentration of 10^5 cells per well in 24-well plates. The following day, we tested anti-FIPV activity of various concentrations of R or RL, which were determined based on the cell viability assay results (Fig. 1B and C).

The cells were pre-treated with various concentrations of R, RL or DMSO(as a vehicle control) for 2 hours before infection with FIPV at a MOI of 0.008 with same concentrations of drug. The cytopathic effect (CPE) induced by the virus was monitored for up to 72 hours. Following this, the supernatant of the cell lysates was collected and subjected to titration or RT-qPCR.

2.6. RNA Extraction and RT-qPCR Assay

Vira RNA was isolated using Viral Gene-spin™ Viral DNA/RNA Extraction Kit (iNtRON, Gyeonggi-do, Korea). To quantify viral RNA, we used the primers and probe set targeting the 3'UTR region of FIP virus from the previous study by modifying reporter fluorescence to FAM [29]. The reaction mixes were prepared using the RNA UltraSense™ One-Step Quantitative RT-PCR System (Thermo Fisher Scientific, Cleveland, OH, USA) according to the manufacturer's guidelines. The prepared mixture was incubated at 50°C for 15 minutes and at 95°C for 2 minutes, followed by 40 repetitions of the reaction at 95°C for 15 seconds and 60°C for 30 seconds using LightCycler® 96 Real-Time PCR System (Roche, Basel, Switzerland). The obtained Cq value was converted into a log($TCID_{50}$/ml) equivalent using a standard curve.

2.7. Western Blot

The CRFK cells ($2x10^5$ cells/ml) were prepared in a 24-well plate and incubated for 24 hours. After removing the medium, the medium containing 1 MOI of FIPV and 2.5μM RL was added. After 15, 30, 45, and 60 minutes, the cell lysates were collected using M-Per® Mammalian Protein Extraction Reagent (Thermo Fisher Scientific, Cleveland, OH, USA), and then cell debris was removed by centrifugation.

For Sodium dodecyl-sulfate polyacrylamide gel electrophoresis (SDS-PAGE), samples were processed with a 4x LDS sample buffer (Thermo Fisher Scientific, Cleveland, OH, USA) according to the manufacturer's guideline. 10μL of the prepared sample was loaded on Bolt™ 4 to 12%, Bis-Tris gel, and electrophoresed at 200 volts for 25 minutes. Then, the bands were transferred to a nitrocellulose membrane under the condition of 20 volts for 1 hour as suggested by the manufacturer. The transferred membrane was washed 3 times with the washing buffer and stained with the primary antibody diluted with blocking buffer. After overnight incubation at 4°C, the membrane was washed 3 times and incubated with the secondary antibody diluted with blocking buffer. After incubation for 2 hours, it was washed 3 times with PBS, and developed using Clarity Western ECL Substrate (BIO-RAD, USA), the images were taken using the FUSION SOLO (Vilber Lourmat, Marne-la-Vallée, France). For β-actin signal, the previously stained membrane was stripped with Restore™ Stripping Buffer (Thermo Fisher Scientific, Cleveland, OH, USA) for 15 minutes and then stained with Anti β-actin antibody, HRP (Abcam, Cambridge, MA, USA) for 2 hours and analyzed. The captured images were quantified by ImageJ [45].

 doi:10.20944/preprints202304.0106.v1

2.8. Time of Addition Assay

Based on virus inoculation time point (+0 hour), seven groups (A to G, Fig. 4A) of the inoculation times of the RL were organized. 24 hours before the inoculation, the $2x10^5$ cells/ml CRFK cells were prepared on a 24-well plate. At a predetermined point, the medium in each well was removed and 2.5 μM of the RL was added. At +0 hours, the medium containing 0.008 MOI of FIPV and 2.5μM RL was added, incubated for 1hr, and removed. The cells were further incubated for up to 72 hours with the media containing 2.5 μM of the RL and the cell lysates were collected. The samples were subjected to titration or qRT-PCR.

2.9. Immunofluorescent Assay

The CRFK cells were prepared at $2x10^5$ cells/ml in a 24-well plate and cultured for 24 hours. After removing the medium, the medium containing 0.008 MOI of FIPV and 2.5μM R or RL was added. After 1 hour, the medium was removed, and the cells were washed with PBS. After that, a medium containing 2.5μM of R or RL was added and cultured for 24 hours. After treatment, the cells were washed once with PBS and then fixed with 4% paraformaldehyde for 15 minutes followed by permeabilizing for 15 minutes using 0.05% triton-X100. After washing 3 times with PBS, the primary antibody diluted with blocking buffer was added to the cells. After overnight incubation at 4°C, the cells were washed three times with washing buffer, and the diluted secondary antibody was added. After incubation for 3 hours, the cells were washed 3 times and mounted. The cells were observed using EVOS® FL Color (Thermo Fisher Scientific, Cleveland, OH, USA). [NO_PRINTED_FORM]The captured images were quantified by ImageJ [45].

2.10. Internalization Assay

The CRFK cells were seeded on a chamber slide at the concentration of $1x10^5$ cells/ml and incubated for 24 hours. The cells were pre-treated with the Rottlerin-Liposome at a concentration of 2.5 μM and incubated for 1 hour. After discarding the medium, the cells were inoculated with a mixture of 1 MOI of FIPV and 2.5 μM of RL. After 1 hour of incubation for viral internalization, the cells were washed and replenished with the media containing 2.5 μM of RL. In the mock test group, a fresh medium containing DMSO was dispensed. After 2, 4, and 6 hours, each well was treated with PBS containing protein kinase (Takara Korea Biomedical Inc., Seoul, Korea) or not for 45 minutes at 4°C and fixed, stained, and observed under or LSM-900 (Carl Zeiss, Göttingen, Germany). Microscopic images were processed by ImageJ software and fluorescence signals were quantified [45]. The fluorescence intensity from at least 50 cells for each group was averaged.

2.11. Statistical Analysis

All statistical analyses were conducted using GraphPad Prism version 8 (GraphPad Software, Inc., San Diego, CA, USA). The 50% cytotoxicity concentrations (CC_{50}) and 50% effective concentrations (CC_{50}) were calculated using a nonlinear regression analysis. Depending on the variable of the data, either one-way ANOVA and Dunnett's multiple comparison or two-way ANOVA and Tukey's multiple comparison were applied. The statistical significance was indicated by the symbols (*), (**), (***), and (****) representing $p<0.05$, $p<0.005$, $p<0.0005$, and $p<0.0001$, respectively.

3. Results

3.1. RL Inhibits FIPV Replication

To investigate the effect of RL on the replication of FIPV in cell culture, we first prepared RL by loaded R into a lipid bilayer vesicle. The shape and the size of RL were confirmed by electron microscopy and dynamic light scattering. 96.3% of the RL had a uniform particle size of 110nm diameter with a spherical shape (Fig. S1). We then evaluated the cytotoxicity of RL on CRFK cells using the Water-Soluble Tetrazolium Salts (WST) assay with serial dilution of each compound. The

Preprints (www.preprints.org) | NOT PEER-REVIEWED | Posted: 7 April 2023 doi:10.20944/preprints202304.0106.v1

50% cytotoxic concentration (CC_{50}) of RL was 3.53 μM, which was similar to R (3.90 μM) (R^2>0.95, Fig. 1A). Next, we determined the inhibitory effects of RL against FIPV in cell culture at concentration below the CC_{50}. CRFK cells pretreated with various concentrations of RL or R and then infected with FIPV (0.008 MOI) in the presence of RL or R. After 72 hours post infection, viral RNA synthesis, N protein expression, and virus titer were measured. As shown in Fig. 1B-D, both RL and R treatment significantly inhibited FIPV replication in dose dependent manner. All tested concentrations showed statistically significant differences compared to mock. The effective concentrations inhibiting 50% viral replication (EC_{50}) of RL and R was 1.40μM and 1.60μM, respectively (R2 > 0.95). Interestingly, RL showed a significantly enhanced antiviral effect ($p<0.05$) compared to R in terms of viral RNA, protein, and titration, suggesting that loading R on a liposome could increase its potency (fig S2). To ensure that the observed antiviral effect of RL was not due to the liposome carrier, we tested the equivalent concentration of the liposome (L) and found that L treatment did not show significant differences from the mock (Fig. 1D, S2), further supporting that the antiviral effect of RL is attributed to R.

3.2. RL Decreased PKC Delta Phosphorylation Induced by FIP Infection at an Ealy Time of Infection

To investigate whether RL inhibit FIPV replication through the PKCδ-dependent or not, we tracked the phosphorylation of PKCδ over time after FIPV infection with or without RL. CRFK cells were infected with a mixture of FIPV (MOI of 1) and RL(2.5μM), and the cell lysates were collected at 15, 30, 45, and 60 minutes after infection for western blotting to measure total PKCδ, phosphorylated PKCδ (PKCδ-S645) and β-actin.

The levels of phosphorylated PCKδ in FIPV-infected groups (FIPV +) were significantly increased compared to those of the negative control group (FIPV - / RL -) at all time points (1.21~1.32, $p<0.0001$, not indicated), suggesting that FIPV infection induced phosphorylation of PCKδ (Fig. 2A and B). Strikingly, the RL-treated group exhibited a decreasing trend in the phosphorylated PKCδ compared to the positive control group (FIPV+/RL-) at 15, 30, and 45 minutes after infection (Fig. 2A and B). Statistical analysis showed that the RL treatment significantly reduced the phosphorylated PKCδ at 15 minutes after infection (FIPV+/RL-, 1.32±0.01 vs. FIPV+/RL+,1.24±0.02, $p<0.05$) (Fig. 2B). These results suggest that RL treatment decreased FIPV-induced PKCδ phosphorylation at an early time of infection.

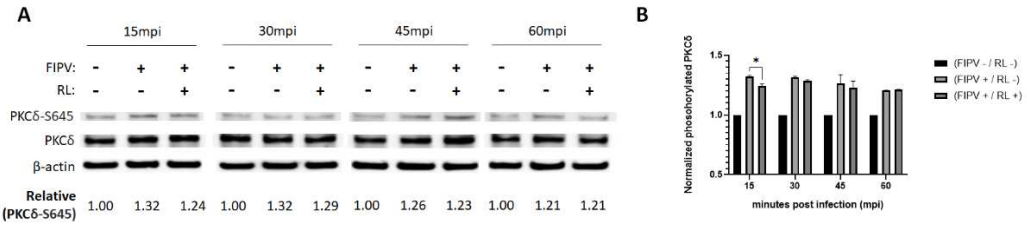

Figure 2. The inhibitory effect of RL on FIPV replication is related to PKCδ activation. Pre-treated (2.5 μM RL for 2 hours) confluent CRFK cells were infected with FIPV (MOI=1) and RL and collected 15, 30, 45, and 60 minutes post infection. **(A)** The cell lysates were subjected to SDS-PAGE for Western blotting. The phosphorylated and total PKCδ were detected using rabbit anti-PKCδ-S645 and rabbit anti-PKCδ antibody, respectively. β-actin was employed as an internal control. Bands was quantified using Image J software, with normalization using the β-actin signal. The intensity of phosphorylated PKCδ was presented as a fold-change relative to the negative control (NC, FIPV - / RL -) of each time point. **(B)** The measured signals were plotted on a graph. Statistical differences were analyzed through two-way ANOVA and Tukey's multiple comparison test, with the symbol (*) indicating $p<0.05$.

3.3. RL Inhibited FIPV Replication at both Early and Late Steps of Infection

To investigate at which stage of FIPV replication is inhibited by RL, a time of addition assay was conducted. The experimental design is presented in Fig. 3A. During the period from -2 to +72 hours,

Preprints (www.preprints.org) | NOT PEER-REVIEWED | Posted: 7 April 2023 doi:10.20944/preprints202304.0106.v1

RL was present in the media as indicated, and FIPV was inoculated from 0 to +1hour. After +72 hours, each cell lysate was collected, and the viral RNA and infectious particle titers were measured. As shown in Fig. 4B and C, RL treatment showed significant inhibition on both viral RNA and infectious virus titer of all time groups compared to mock groups ($p< 0.0001$ or $p<0.0005$). RL pre-treatment at -2 (group A) showed the highest reduction in viral RNA [4.7±0.5log ($TCID_{50}$/ml) equivalent] and titer [5.2±0.1log($TCID_{50}$/ml)] among all groups, suggesting that RL affects an early stage of FIPV infection. RL treatment at +0, +1, +3, +5, and +9 (Group B, C, D, E, and F) resulted in intermediate inhibition of viral replication. Interestingly, RL treatment at +24 hours (group G) significantly decreased viral titer but only slightly decreased viral RNA, indicating that the RL affect a late step of FIPV infection, which could be associated with disrupting viral protein translation, capsid assembly, virus release, or spread.

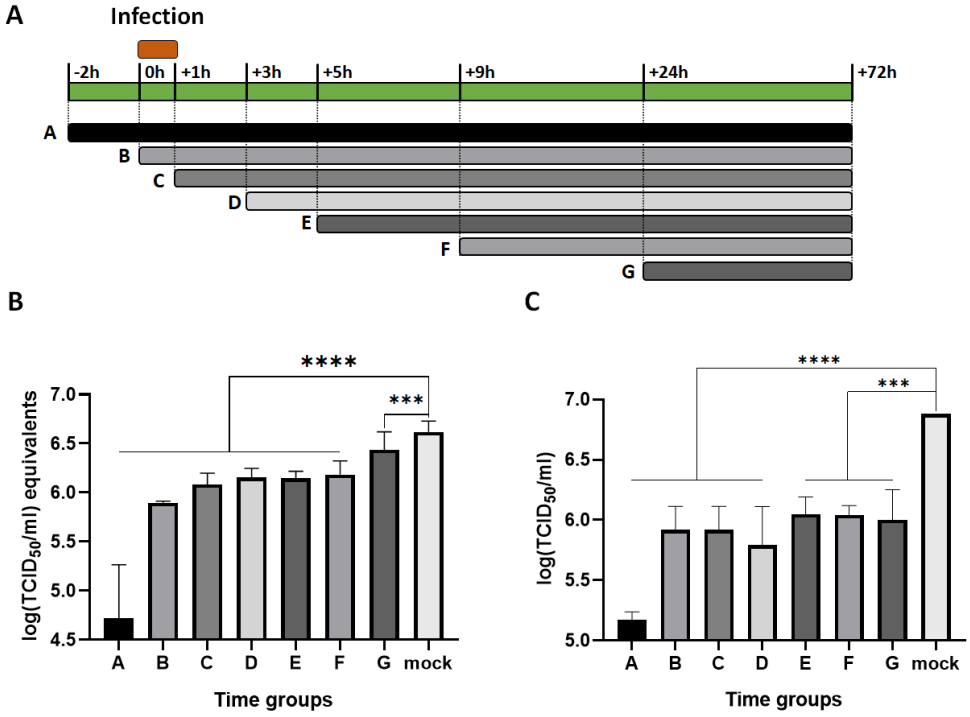

Figure 3. The RL exhibits inhibitory effects at least two deferent stages of FIPV replication. Confluent CRFK cells were infected with FIPV (MOI = 0.008) from +0 to +1 hour. RL (2.5 μM) was existed in the media at an indicated time point. **(A)** The schematic diagram of the time of addition assay. **(B)** The cell lysates were subjected to extract viral RNA for RT-qPCR. The Cq values were converted into log (TCID50/ml) equivalent with standard curve. **(C)** Production of infectious virus was quantified and presented as log (TCID50/ml). The statistical differences were analyzed by one-way ANOVA and Dunnett's multiple comparison. The symbols (****) and (***) indicate $p<0.0001$ and $p<0.0005$, respectively.

3.4. RL Decreased FIPV-Mediated Syncytia in Cell Culture

To explore the effect of RL on the FIPV growth pattern in the CRFK cells, we utilized the immunofluorescence assay to observed virus-infected cells in the presence or absence of RL. As expected, both RL and R treatment resulted in a decrease in the number and intensity of signals compared to the mock and liposome controls. This is consistent with the the titration and Western blot results (Fig. 1), confirming that RL inhibited FIPV replication (Fig.4A). In quantification analysis, both RL($1.4x10^7$±4.0^6) and R($1.8x10^7$±$2.8x10^6$) showed significantly lower fluorescence intensity than mock($2.2x10^7$±$3.9x10^6$) or Liposome ($2.3x10^7$±$2.5x10^6$)(Fig. 4A). Surprisingly, RL and R treated cells showed fewer syncytia formations than the mock and liposome-treated cells. To quantify our observation, we counted the average number of nuclei per syncytium, which is an indication of cell-

Preprints (www.preprints.org) | NOT PEER-REVIEWED | Posted: 7 April 2023 doi:10.20944/preprints202304.0106.v1

cell fusion formation [46]. The average number of nuclei per syncytium of both RL (3.37) and R (2.92) treated cells were significantly lower than mock (11.29) and Liposome (10.58) (Fig. 4B). These results indicate that RL might interfere with syncytia formation by FIPV at a late stage of infection.

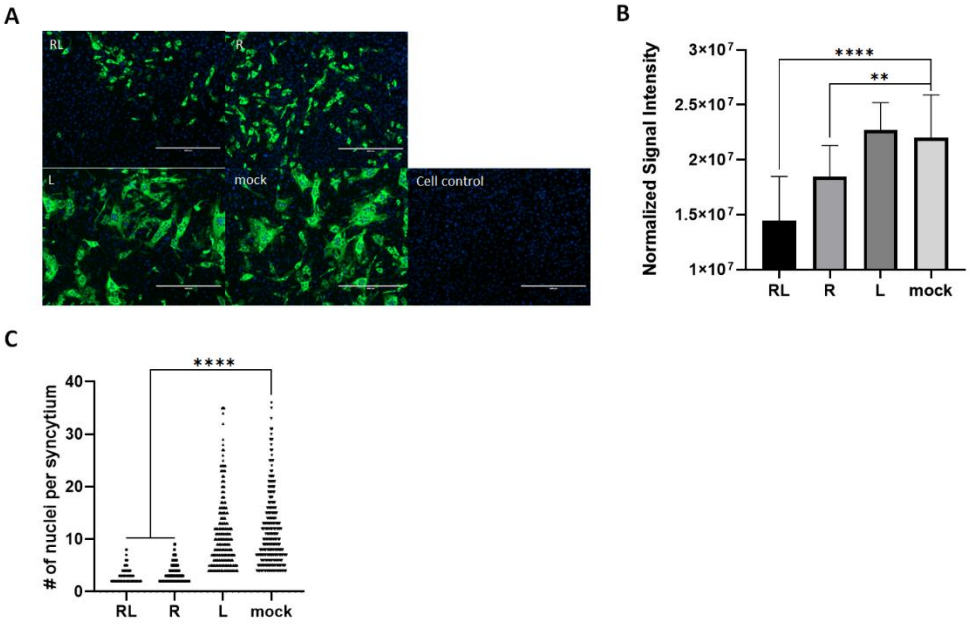

Figure 4. The Rottlerin decreased syncytial fomation by FIP. (A) Confluent CRFK cells were infected with FIPV(MOI=0.008) and 2.5 μM of R, RL or L for 24 hours. Then, the cells were fixed, and FIPV N protein was stained. The stained cells were observed under a fluorescence microscope (green=FIPV N protein, blue=nuclei). The captured images were quantified, and the intensity of the green fluorescence signal per cells was plotted (right). **(B)** The number of nuclei per syncytium (NPS) was quantified. The symbols (****) and (**) indicate $p<0.0001$ and $p< 0.005$.

3.5. The RL Inhibits FIPV Endocytosis

Since pre-treatment of RL showed the most significant reduction of FIPV replication, we hypnotized that RL treatment could disturb the entry process of FIPV. To test this hypothesis, we observed the early localization of FIPV in CRFK cells after treatment of RL or mock (DMSO) with or without proteinase K(proK). The proK treatment is capable of removing outside viruses on the plasma membrane, thereby enabling us to observe endocytosed virus particles (Fig. 5). Two hours post infection, the mock group showed no difference in fluorescence signal intensity between with and without proK treatment. Strikingly, RL treatment significantly reduced the fluorescence signal intensity after proK treatment, suggesting that RL inhibits endocytosis of FIPV (Fig. 5A and B). At four and six hours post infection, RL treatment resulted in significant reduction in fluorescence signal intensity compared to mock-treated cells, which is consistent with the previous results (Fig. 5C and D). These results indicate that the RL can inhibit the endocytosis of FIPV at an early step of replication.

Preprints (www.preprints.org) | NOT PEER-REVIEWED | Posted: 7 April 2023 doi:10.20944/preprints202304.0106.v1

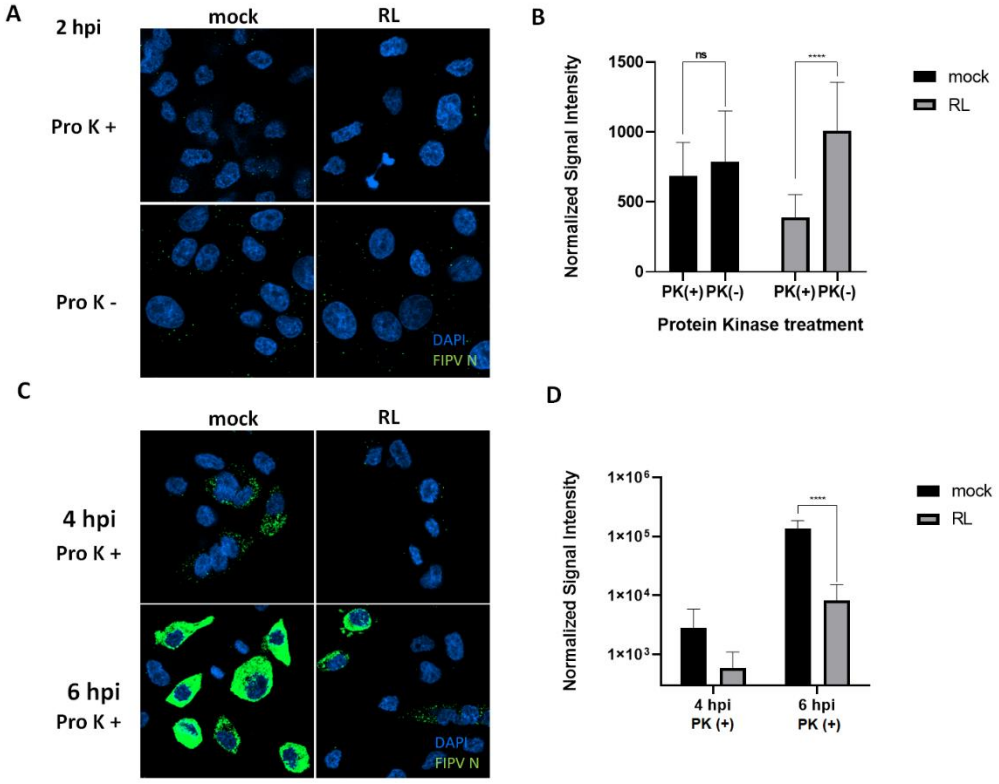

Figure 5. RL inhibited Internalization (or endosomal exit) of FIPV. (A and B) After treating confluent CRFK cells with the RL(2.5 μM) for 2hours, a mixture of RL(2.5 μM) and FIPV(MOI=0.008) was inoculated for 1hour and replenished with fresh media with RL. After 2 hours post infection, the cells were treated with Proteinase K(Pro K+) or PBS(Pro K -) for 45 minutes, fixed and stained. The cells were analyzed by confocal microscopy (green=FIPV N, blue=nuclei). The intensity of green signal per cells were quantified from taken images by Image J and plotted. **(C and D)** As in panel A except incubation for 4 and 6 hours. The cells were proteinase K treated for 45 minutes. The symbols (ns) and (****) indicate $p>0.05$ and $p< 0.0001$.

4. Discussion

In this study, we presented preliminary evidence that RL has inhibitory activity against FIPV in CRFK cells. R has been shown antiviral activity against many viruses, especially enveloped viruses including Chikungunya Virus, Dengue virus, Human Immunodeficiency Virus-1(HIV-1), Human T-cell Leukemia Virus-1(HTLV-1), La crosse virus, Porcine Reproductive and Respiratory Syndrome Virus (PRRSV), Rabies virus, Rift valley fever virus, SARS-CoV-2, and ZIKA virus [4,5,8,12,13,47–50]. These results raise the possibility for considering R as a broad-spectrum antiviral for emergency usage against potential future viral outbreaks.

We presented that RL inhibited the replication of FIPV by interrupting its endocytosis (Fig. 5). This effect appears to be closely related to the reduction in phosphorylation of PKCδ (Fig. 2). These findings are corroborated by the time of addition assay, which revealed that the greatest inhibition of FIPV replication was achieved with pretreatment of RL(Fig3). Notably, inhibition of viral endocytosis by R has also been reported in other viruses, including PRRSV, Zika virus, and puumalavirus [4,8,51]. This endocytosis blocking by R can happen through the regulation of actin cytoskeleton by inactivating PKCδ by R, as the actin cytoskeleton is crucial for various forms of endocytosis, such as clathrin-mediated endocytosis and micropinocytosis [52,53]. The regulation of PKCδ can modulate actin rearrangement, thus impacting viral endocytosis.

We have presented evidence demonstrating that RL inhibits also late step of FIPV replication. Treatment with R and RL on FIPV-infected cells resulted in a reduction in the number of syncytia formed (Fig. 4). Furthermore, the time of addition assay showed that viral titer ($TCID_{50}$/ml) was

 doi:10.20944/preprints202304.0106.v1

significantly more inhibited than viral RNA ($TCID_{50}$ /ml equivalents) at +24h (Fig. 3). Based on these results, we infer that RL inhibits downstream steps from viral RNA synthesis. Two possible hypotheses may explain the effect of R on the late stage of FIPV replication and syncytia formation. Firstly, R may affect the process of protein synthesis from viral RNA, as it has been shown to inhibit the translation of viral mRNA [9,54]. Second, R may directly or indirectly inhibit the function of the spike protein or fusion-related factors, as similar to drugs such as EK1 and Abl kinase inhibitors [46,55]. To determine the underlying mechanism of R at late step of FIPV replication, we plan to conduct more detailed future studies by transfecting the mRNA encoding FIPV's S protein together with RL or by treating the cells with externally synthesized S protein with RL[56].

Taken together, these results suggest that R may inhibit FIPV replication via two distinct steps: an early step involving endocytosis and a late step involving viral protein synthesis or spread. Interestingly, R has been shown to exert antiviral effects against various viruses through PKCδ-dependent pathways (such as HIV-1 and PRRSV), or PKCδ-independent pathways that reduce ATP levels (such as Rabies virus), suggesting R may inhibit multiple steps of viral replication [4,5,49]. This finding is consistent with a recent Zika virus report that R disrupts both endocytosis and late-stage replication by interfering with the virus maturation [8]. Nonetheless, the underlying mechanism by which R blocks multiple steps in some enveloped viruses require further investigation.

We demonstrated the advantages of liposome in enhancing the potency of R (Fig. 1 and 4). Liposomes offer additional advantages for clinical use of R. First, liposome-based formulations can overcome challenges related to solubility, bioavailability, pharmacological activity, stability, distribution, and sustained delivery of natural extracts [19,20]. Thus, liposomes are widely used in the field of natural extracts, like R, with various combinations of lipids and size [57]. The RL we made in this study could accommodate a maximum of 2.5mg/ml of R, providing us with a sufficient drug concentration in small volume for future in vivo studies. Second, RL could increase its uptake by macrophages, which could enhance its antiviral effect against FIPV. Liposomes with a size under 100nm are known to facilitate their uptake by macrophages [58]. FIPV infection in macrophages causes pathogenesis of FIP characterized by the release of inflammatory factors from macrophages that lead to vessel leakage and the formation of granulomatous lesions [25,59,60]. Thus, if RL can specifically target macrophages, it may not only increase the efficiency of R but also decrease its toxicity. Hence, it is worthwhile to investigate the application of liposomes to R or other anti-FIP drugs and evaluate their positive effects through in vivo studies.

The 50% cytotoxic concentration (CC_{50}) values of R and RL measured in CRFK cells were 3.90 and 3.53μM, respectively, which is lower than that of other known small molecule inhibitors (Fig. 1). The CC_{50} values of other compounds effective against FIPV ranged from 5.99μM to 515.7μM in various cell models [16,38–40,61–63]. These results raise safety concern, as evaluating the safety of chemical substances during the development into pharmaceuticals is crucial [24]. However, direct comparison of their CC_{50} values among different studies might be unreasonable due to differences in the cell models used. For example, when the R was used in other studies with A549 cells or Vero cells, their CC_{50} value was 47.78μM and 11.24μM, respectively [8,48]. In a previous pig study conducted by our group, a dose of 1mg/pig did not cause any observed adverse effects [4]. While toxicity evaluations consistent with pharmaceutical safety assessment guidelines must be conducted, we anticipate no obstacles in developing RL as a pharmaceutical composition.

5. Conclusions

In this study, we demonstrated that RL efficiently inhibited FIPV replication in cell culture by reducing of FIPV endocytosis. RL decreased FIPV-induced PKCδ phosphorylation at an early step of infection. We observed that RL reduced both fluorescent signals for FIPV N protein and the formation of syncytia in FIPV infected cells. Throughout the test, liposome enhanced the potency of R. These results suggest that RL has the potential to be further investigated for its antiviral activity.

Supplementary Materials: The following supporting information can be downloaded at the website of this paper posted on Preprints.org.

Author Contributions: Conceptualization, C. O., J.-C.C., D.-H.L., S.-W.L., S.-Y.P., C.-S.S., I.-S.C. and Y.-L.K.; methodology, C. O. and J.-C.C.; software, J.-C.C.; validation, C. O. and J.-C.C.; formal analysis, J.-C.C.; investigation, J.-C.C., S.-W.J., I.-Y.C.; resources, S.-W.J. and I.-Y.C.; data curation, J.-C.C.; writing—original draft preparation, C. O. and J.-C.C.; writing—review and editing, C. O. and J.-C.C.; visualization, J.-C.C.; supervision, C. O.; project administration, C. O. and J.-C.C.; funding acquisition, J.-C.C. All authors have read and agreed to the published version of the manuscript.

Funding: This work was supported by Korea Institute of Planning and Evaluation for Technology in Food, Agriculture and Forestry (IPET) through Animal disease Management Technology Development Program (121004-1) and Agriculture, Food, and Rural Affairs Convergence Technologies Program for Educating Creative Global Leader Program (320005-04-4-SB080), funded by Ministry of Agriculture, Food, and Rural Affairs (MAFRA).

Data Availability Statement: Data are available from the corresponding author upon reasonable request.

Acknowledgments: We express our deepest gratitude to the KU Research Center for Zoonosis for providing advice on the design and progress of the study.

Conflicts of Interest: J.-C.C. is employees of Qvet (Seoul, Korea). The rest of the authors declare that they have no relevant conflict of interest.

References

1. Kumar, A.; Patil, M.; Kumar, P.; Bhatti, R.C.; Kaur, R.; Sharma, N.K.; Singh, A.N. Mallotus Philippensis (Lam.) Müll. Arg.: A Review on Its Pharmacology and Phytochemistry. *Journal of HerbMed Pharmacology* 2021, *10*, 31–50.
2. Rivière, C.; Nguyen Thi Hong, V.; Tran Hong, Q.; Chataigné, G.; Nguyen Hoai, N.; Dejaegher, B.; Tistaert, C.; Nguyen Thi Kim, T.; Vander Heyden, Y.; Chau Van, M.; et al. Mallotus Species from Vietnamese Mountainous Areas: Phytochemistry and Pharmacological Activities. *Phytochemistry Reviews* 2010, *9*, 217–253.
3. Gschwendt, M.; Muller, H.J.; Kielbassa, K.; Zang, R.; Kittstein, W.; Rincke, G.; Marks, F. Rottlerin, a Novel Protein Kinase Inhibitor. *Biochem Biophys Res Commun* **1994**, *199*, 93–98, doi:10.1006/bbrc.1994.1199.
4. Kang, Y.L.; Oh, C.; Ahn, S.H.; Choi, J.C.; Choi, H.Y.; Lee, S.W.; Choi, I.S.; Song, C.S.; Lee, J.B.; Park, S.Y. Inhibition of Endocytosis of Porcine Reproductive and Respiratory Syndrome Virus by Rottlerin and Its Potential Prophylactic Administration in Piglets. *Antiviral Res* **2021**, *195*, doi:10.1016/j.antiviral.2021.105191.
5. Contreras, X.; Mzoughi, O.; Gaston, F.; Peterlin, M.B.; Bahraoui, E. Protein Kinase C-Delta Regulates HIV-1 Replication at an Early Post-Entry Step in Macrophages. *Retrovirology* **2012**, *9*, 37, doi:10.1186/1742-4690-9-37.
6. Zhao, H.; Guo, X.; Bi, Y.; Zhu, Y.; Feng, W. PKCδ Is Required for Porcine Reproductive and Respiratory Syndrome Virus Replication. *Virology* **2014**, *468–470*, 96–103, doi:10.1016/j.virol.2014.07.040.
7. Manhas, D.; Gour, A.; Bhardwaj, N.; Sharma, D.K.; Sharma, K.; Vij, B.; Jain, S.K.; Singh, G.; Nandi, U. Pharmacokinetic Assessment of Rottlerin from Mallotus Philippensis Using a Highly Sensitive Liquid Chromatography-Tandem Mass Spectrometry-Based Bioanalytical Method. *ACS Omega* **2021**, *6*, 32637–32646, doi:10.1021/acsomega.1c04266.
8. Zhou, S.; Lin, Q.; Huang, C.; Luo, X.; Tian, X.; Liu, C.; Zhang, P. Rottlerin Plays an Antiviral Role at Early and Late Steps of Zika Virus Infection. *Virol Sin* **2022**, *37*, 685–694, doi:10.1016/j.virs.2022.07.012.
9. Ietta, F.; Maioli, E.; Daveri, E.; Gonzaga Oliveira, J.; da Silva, R.J.; Romagnoli, R.; Cresti, L.; Maria Avanzati, A.; Paulesu, L.; Barbosa, B. de F.; et al. Rottlerin-Mediated Inhibition of Toxoplasma Gondii Growth in BeWo Trophoblast-like Cells. *Sci Rep* **2017**, *7*, 1279, doi:10.1038/s41598-017-01525-6.
10. Pandey, S.; Chatterjee, A.; Jaiswal, S.; Kumar, S.; Ramachandran, R.; Srivastava, K.K. Protein Kinase C-δ Inhibitor, Rottlerin Inhibits Growth and Survival of Mycobacteria Exclusively through Shikimate Kinase. *Biochem Biophys Res Commun* **2016**, *478*, 721–726, doi:10.1016/j.bbrc.2016.08.014.
11. Shivshankar, P.; Lei, L.; Wang, J.; Zhong, G. Rottlerin Inhibits Chlamydial Intracellular Growth and Blocks Chlamydial Acquisition of Sphingolipids from Host Cells. *Appl Environ Microbiol* **2008**, *74*, 1243–1249, doi:10.1128/AEM.02151-07.
12. Filone, C.M.; Hanna, S.L.; Caino, M.C.; Bambina, S.; Doms, R.W.; Cherry, S. Rift Valley Fever Virus Infection of Human Cells and Insect Hosts Is Promoted by Protein Kinase C Epsilon. *PLoS One* **2010**, *5*, e15483, doi:10.1371/journal.pone.0015483.
13. MORI, N.; ISHIKAWA, C.; SENBA, M. Activation of PKC-δ in HTLV-1-Infected T Cells. *Int J Oncol* **2015**, *46*, 1609–1618, doi:10.3892/ijo.2015.2848.

14. Gao, A.; Hu, X. li; Saeed, M.; Chen, B. fan; Li, Y. ping; Yu, H. jun Overview of Recent Advances in Liposomal Nanoparticle-Based Cancer Immunotherapy. *Acta Pharmacol Sin* 2019, *40*, 1129–1137.
15. Gheibi Hayat, S.M.; Darroudi, M. Nanovaccine: A Novel Approach in Immunization. *J Cell Physiol* 2019.
16. Hu, C.M.J.; Chang, W.S.; Fang, Z.S.; Chen, Y.T.; Wang, W.L.; Tsai, H.H.; Chueh, L.L.; Takano, T.; Hohdatsu, T.; Chen, H.W. Nanoparticulate Vacuolar ATPase Blocker Exhibits Potent Host-Targeted Antiviral Activity against Feline Coronavirus. *Sci Rep* **2017**, *7*, 1–11, doi:10.1038/s41598-017-13316-0.
17. Malam, Y.; Loizidou, M.; Seifalian, A.M. Liposomes and Nanoparticles: Nanosized Vehicles for Drug Delivery in Cancer. *Trends Pharmacol Sci* 2009, *30*, 592–599.
18. Qi, X.-R.; Zhao; Zhuang Comparative Study of the in Vitro and in Vivo Characteristics of Cationic and Neutral Liposomes. *Int J Nanomedicine* **2011**, 3087, doi:10.2147/ijn.s25399.
19. Sogut, O.; Aydemir Sezer, U.; Sezer, S. Liposomal Delivery Systems for Herbal Extracts. *J Drug Deliv Sci Technol* **2021**, *61*, 102147, doi:10.1016/j.jddst.2020.102147.
20. Olusanya, T.; Haj Ahmad, R.; Ibegbu, D.; Smith, J.; Elkordy, A. Liposomal Drug Delivery Systems and Anticancer Drugs. *Molecules* **2018**, *23*, 907, doi:10.3390/molecules23040907.
21. Chang, Y.; Meng, F.-C.; Wang, R.; Wang, C.M.; Lu, X.-Y.; Zhang, Q.-W. Chemistry, Bioactivity, and the Structure-Activity Relationship of Cephalotaxine-Type Alkaloids From Cephalotaxus Sp. In; 2017; pp. 339–373.
22. De Rosa, G.; Campani, V.; Marchese, D.; Pitaro, M.T.; Pitaro, M.; Grieco, P. Development of a Liposome-Based Formulation for Vitamin K1 Nebulization on the Skin. *Int J Nanomedicine* **2014**, 1823, doi:10.2147/IJN.S58365.
23. Zou, L.; Liu, W.; Liu, W.; Liang, R.; Li, T.; Liu, C.; Cao, Y.; Niu, J.; Liu, Z. Characterization and Bioavailability of Tea Polyphenol Nanoliposome Prepared by Combining an Ethanol Injection Method with Dynamic High-Pressure Microfluidization. *J Agric Food Chem* **2014**, *62*, 934–941, doi:10.1021/jf402886s.
24. Kim, Y.; Shivanna, V.; Narayanan, S.; Prior, A.M.; Weerasekara, S.; Hua, D.H.; Kankanamalage, A.C.G.; Groutas, W.C.; Chang, K.-O. Broad-Spectrum Inhibitors against 3C-Like Proteases of Feline Coronaviruses and Feline Caliciviruses. *J Virol* **2015**, *89*, 4942–4950, doi:10.1128/jvi.03688-14.
25. Rottier, P.J.M.; Nakamura, K.; Schellen, P.; Volders, H.; Haijema, B.J. Acquisition of Macrophage Tropism during the Pathogenesis of Feline Infectious Peritonitis Is Determined by Mutations in the Feline Coronavirus Spike Protein. *J Virol* **2005**, *79*, 14122–14130, doi:10.1128/jvi.79.22.14122-14130.2005.
26. Chang, H.W.; Egberink, H.F.; Halpin, R.; Spiro, D.J.; Rottie, P.J.M. Spike Protein Fusion Peptide and Feline Coronavirus Virulence. *Emerg Infect Dis* **2012**, *18*, 1089–1095, doi:10.3201/eid1807.120143.
27. Pedersen, N.C. An Update on Feline Infectious Peritonitis: Diagnostics and Therapeutics. *Veterinary Journal* 2014, *201*, 133–141.
28. Pedersen, N.C.; Eckstrand, C.; Liu, H.; Leutenegger, C.; Murphy, B. Levels of Feline Infectious Peritonitis Virus in Blood, Effusions, and Various Tissues and the Role of Lymphopenia in Disease Outcome Following Experimental Infection. *Vet Microbiol* **2015**, *175*, 157–166, doi:10.1016/j.vetmic.2014.10.025.
29. Kim, Y.; Liu, H.; Galasiti Kankanamalage, A.C.; Weerasekara, S.; Hua, D.H.; Groutas, W.C.; Chang, K.O.; Pedersen, N.C. Reversal of the Progression of Fatal Coronavirus Infection in Cats by a Broad-Spectrum Coronavirus Protease Inhibitor. *PLoS Pathog* **2016**, *12*, doi:10.1371/journal.ppat.1005531.
30. Ritz, S.; Egberink, H.; Hartmann, K. Effect of Feline Interferon-Omega on the Survival Time and Quality of Life of Cats with Feline Infectious Peritonitis. *J Vet Intern Med* **2007**, *21*, 1193–1197, doi:10.1892/06-302.1.
31. Fischer, Y.; Ritz, S.; Weber, K.; Sauter-Louis, C.; Hartmann, K. Randomized, Placebo Controlled Study of the Effect of Propentofylline on Survival Time and Quality of Life of Cats with Feline Infectious Peritonitis. *J Vet Intern Med* **2011**, *25*, 1270–1276, doi:10.1111/j.1939-1676.2011.00806.x.
32. Legendre, A.M.; Bartges, J.W. Effect of Polyprenyl Immunostimulant on the Survival Times of Three Cats with the Dry Form of Feline Infectious Peritonitis. *J Feline Med Surg* **2009**, *11*, 624–626, doi:10.1016/j.jfms.2008.12.002.
33. Addie, D.D.; Paltrinieri, S.; Pedersen, N.C. Recommendations from Workshops of the Second International Feline Coronavirus/Feline Infectious Peritonitis Symposium. In Proceedings of the Journal of Feline Medicine and Surgery; W.B. Saunders Ltd, 2004; Vol. 6, pp. 125–130.
34. Addie, D.; Belák, S.; Boucraut-Baralon, C.; Egberink, H.; Frymus, T.; Gruffydd-Jones, T.; Hartmann, K.; Hosie, M.J.; Lloret, A.; Lutz, H.; et al. Feline Infectious Peritonitis: ABCD Guidelines on Prevention and Management. *J Feline Med Surg* **2009**, *11*, 594–604, doi:10.1016/j.jfms.2009.05.008.
35. Takano, T.; Katoh, Y.; Doki, T.; Hohdatsu, T. Effect of Chloroquine on Feline Infectious Peritonitis Virus Infection in Vitro and in Vivo. *Antiviral Res* **2013**, *99*, 100–107, doi:10.1016/j.antiviral.2013.04.016.
36. Pedersen, N.C.; Perron, M.; Bannasch, M.; Montgomery, E.; Murakami, E.; Liepnieks, M.; Liu, H. Efficacy and Safety of the Nucleoside Analog GS-441524 for Treatment of Cats with Naturally Occurring Feline Infectious Peritonitis. *J Feline Med Surg* **2019**, *21*, 271–281, doi:10.1177/1098612X19825701.

37. Weiss, R.C.; Oostrom-Ram, T. Inhibitory Effects of Ribavirin Alone or Combined with Human Alpha Interferon on Feline Infectious Peritonitis Virus Replication in Vitro. *Vet Microbiol* **1989**, *20*, 255–265, doi:10.1016/0378-1135(89)90049-7.
38. Doki, T.; Tarusawa, T.; Hohdatsu, T.; Takano, T. In Vivo Antiviral Effects of U18666A Against Type I Feline Infectious Peritonitis Virus. *Pathogens* **2020**, *9*, 67, doi:10.3390/pathogens9010067.
39. Takano, T.; Akiyama, M.; Doki, T.; Hohdatsu, T. Antiviral Activity of Itraconazole against Type I Feline Coronavirus Infection. *Vet Res* **2019**, *50*, 5, doi:10.1186/s13567-019-0625-3.
40. Delaplace, M.; Huet, H.; Gambino, A.; Le Poder, S. Feline Coronavirus Antivirals: A Review. *Pathogens* **2021**, *10*, 1150, doi:10.3390/pathogens10091150.
41. Pedersen, N.C.; Evermann, J.F.; McKeirnan, A.J.; Ott, R.L. Pathogenicity Studies of Feline Coronavirus Isolates 79-1146 and 79-1683. *Am J Vet Res* **1984**, *45*, 2580–2585.
42. Stranieri, A.; Giordano, A.; Paltrinieri, S.; Giudice, C.; Cannito, V.; Lauzi, S. Comparison of the Performance of Laboratory Tests in the Diagnosis of Feline Infectious Peritonitis. *Journal of Veterinary Diagnostic Investigation* **2018**, *30*, 459–463, doi:10.1177/1040638718756460.
43. Wang, R.; Yang, L.; Zhang, Y.; Li, J.; Xu, L.; Xiao, Y.; Zhang, Q.; Bai, L.; Zhao, S.; Liu, E.; et al. Porcine Reproductive and Respiratory Syndrome Virus Induces HMGB1 Secretion via Activating PKC-Delta to Trigger Inflammatory Response. *Virology* **2018**, *518*, 172–183, doi:10.1016/j.virol.2018.02.021.
44. Mahapatra, A.; Kumar, P.; Bhansare, J.; Surapaneni, S.M.; Sen, A.; Pradhan, B. Development of Dye-Sensitized Solar Cell Using M. Philippensis (Kamala Tree) Fruit Extract: A Combined Experimental and Theoretical Study. *Int J Energy Res* **2021**, *45*, 21509–21515, doi:10.1002/er.7153.
45. Schneider, C.A.; Rasband, W.S.; Eliceiri, K.W. NIH Image to ImageJ: 25 Years of Image Analysis. *Nat Methods* **2012**, *9*, 671–675, doi:10.1038/nmeth.2089.
46. Sisk, J.M.; Frieman, M.B.; Machamer, C.E. Coronavirus S Protein-Induced Fusion Is Blocked Prior to Hemifusion by Abl Kinase Inhibitors. *Journal of General Virology* **2018**, *99*, 619–630, doi:10.1099/jgv.0.001047.
47. Abdelnabi, R.; Amrun, S.N.; Ng, L.F.P.; Leyssen, P.; Neyts, J.; Delang, L. Protein Kinases C as Potential Host Targets for the Inhibition of Chikungunya Virus Replication. *Antiviral Res* **2017**, *139*, 79–87, doi:10.1016/j.antiviral.2016.12.020.
48. Ojha, D.; Winkler, C.W.; Leung, J.M.; Woods, T.A.; Chen, C.Z.; Nair, V.; Taylor, K.; Yeh, C.D.; Tawa, G.J.; Larson, C.L.; et al. Rottlerin Inhibits La Crosse Virus-Induced Encephalitis in Mice and Blocks Release of Replicating Virus from the Golgi Body in Neurons. *Nat Microbiol* **2021**, *6*, 1398–1409, doi:10.1038/s41564-021-00968-y.
49. Lama, Z.; Gaudin, Y.; Blondel, D.; Lagaudrière-Gesbert, C. Kinase Inhibitors Tyrphostin 9 and Rottlerin Block Early Steps of Rabies Virus Cycle. *Antiviral Res* **2019**, *168*, 51–60, doi:10.1016/j.antiviral.2019.04.014.
50. Chen, F.; Shi, Q.; Pei, F.; Vogt, A.; Porritt, R.A.; Garcia, G.; Gomez, A.C.; Cheng, M.H.; Schurdak, M.E.; Liu, B.; et al. A Systems-level Study Reveals Host-targeted Repurposable Drugs against SARS-CoV-2 Infection. *Mol Syst Biol* **2021**, *17*, doi:10.15252/msb.202110239.
51. Bauherr, S.; Larsberg, F.; Petrich, A.; Sperber, H.S.; Klose-Grzelka, V.; Luckner, M.; Azab, W.; Schade, M.; Höfer, C.T.; Lehmann, M.J.; et al. Macropinocytosis and Clathrin-Dependent Endocytosis Play Pivotal Roles for the Infectious Entry of Puumala Virus. *J Virol* **2020**, *94*, doi:10.1128/JVI.00184-20.
52. Galletta, B.J.; Mooren, O.L.; Cooper, J.A. Actin Dynamics and Endocytosis in Yeast and Mammals. *Curr Opin Biotechnol* **2010**, *21*, 604–610, doi:10.1016/j.copbio.2010.06.006.
53. Singla, B.; Lin, H.-P.; Ghoshal, P.; Cherian-Shaw, M.; Csányi, G. PKCδ Stimulates Macropinocytosis via Activation of SSH1-Cofilin Pathway. *Cell Signal* **2019**, *53*, 111–121, doi:10.1016/j.cellsig.2018.09.018.
54. Maioli, E.; Torricelli, C.; Valacchi, G. Rottlerin and Cancer: Novel Evidence and Mechanisms. *The Scientific World Journal* **2012**, *2012*, 1–11, doi:10.1100/2012/350826.
55. Xia, S.; Yan, L.; Xu, W.; Agrawal, A.S.; Algaissi, A.; Tseng, C.-T.K.; Wang, Q.; Du, L.; Tan, W.; Wilson, I.A.; et al. A Pan-Coronavirus Fusion Inhibitor Targeting the HR1 Domain of Human Coronavirus Spike. *Sci Adv* **2019**, *5*, doi:10.1126/sciadv.aav4580.
56. Yoo, D.; Parker, M.D.; Babiuk, L.A. The S2 Subunit of the Spike Glycoprotein of Bovine Coronavirus Mediates Membrane Fusion in Insect Cells. *Virology* **1991**, *180*, 395–399, doi:10.1016/0042-6822(91)90045-D.
57. Rahman, H.S.; Othman, H.H.; Hammadi, N.I.; Yeap, S.K.; Amin, K.M.; Abdul Samad, N.; Alitheen, N.B. Novel Drug Delivery Systems for Loading of Natural Plant Extracts and Their Biomedical Applications. *Int J Nanomedicine* **2020**, *15*, 2439–2483, doi:10.2147/IJN.S227805.
58. Kelly, C.; Jefferies, C.; Cryan, S.-A. Targeted Liposomal Drug Delivery to Monocytes and Macrophages. *J Drug Deliv* **2011**, *2011*, 1–11, doi:10.1155/2011/727241.
59. Shah, K.K.; Pritt, B.S.; Alexander, M.P. Histopathologic Review of Granulomatous Inflammation. *J Clin Tuberc Other Mycobact Dis* **2017**, *7*, 1–12, doi:10.1016/j.jctube.2017.02.001.
60. Epstein, W.L.; Fukuyama, K. Mechanisms of Granulomatous Inflammation. *Immunol Ser* **1989**, *46*, 687–721.

61. Barlough, J.; Shacklett, B. Antiviral Studies of Feline Infectious Peritonitis Virus in Vitro. *Veterinary Record* **1994**, *135*, 177–179, doi:10.1136/vr.135.8.177.
62. Hsieh, L.E.; Lin, C.N.; Su, B.L.; Jan, T.R.; Chen, C.M.; Wang, C.H.; Lin, D.S.; Lin, C.T.; Chueh, L.L. Synergistic Antiviral Effect of Galanthus Nivalis Agglutinin and Nelfinavir against Feline Coronavirus. *Antiviral Res* **2010**, *88*, 25–30, doi:10.1016/j.antiviral.2010.06.010.
63. Infection, C.; Takano, T.; Satoh, K.; Doki, T.; Tanabe, T.; Hohdatsu, T. Viruses Antiviral E Ff Ects of Hydroxychloroquine and Type I Interferon on In Vitro Fatal Feline. **2020**, 1–9.